Dymore User's Manual

Formulation and finite element implementation of constraint elements

Contents

1 The lower pair joints

A distinguishing feature of multibody systems is the presence of joints that impose constraints on the relative motion of the various bodies of the system. Most joints used in practical applications can be modeled in terms of the so called *lower pairs* [1]: the revolute, prismatic, screw, cylindrical, planar and spherical joints, depicted in fig. 1. In some cases, however, joints with specialized kinematic conditions must also be developed.

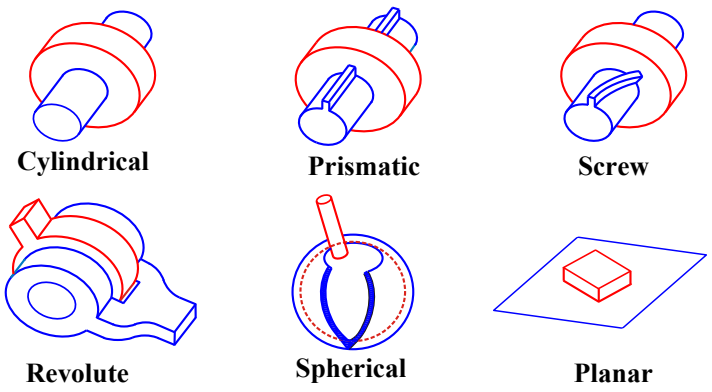

Figure 1: The six lower pairs.

1.1 Kinematics of a typical lower pair joint

Consider two bodies, denoted "body k" and "body ℓ," as shown in fig. 2. Quantities pertaining to body k and body ℓ will be indicated with superscripts $(\cdot)^k$ and $(\cdot)^\ell$, respectively. A lower pair joint, *i.e.*, anyone of the joints depicted in fig. 1, connects the two bodies at points **K** and **L**, which are material points of bodies k and ℓ, respectively. In the reference configuration, two frames, $\mathcal{F}_0^k = \left[\mathbf{K}, \mathcal{B}_0^k = (\bar{e}_{01}^k, \bar{e}_{02}^k, \bar{e}_{03}^k)\right]$ and $\mathcal{F}_0^\ell = \left[\mathbf{L}, \mathcal{B}_0^\ell = (\bar{e}_{01}^\ell, \bar{e}_{02}^\ell, \bar{e}_{03}^\ell)\right]$, are attached to bodies k and ℓ, respectively. In the deformed configuration, the bodies are defined by two frames, $\mathcal{F}^k = \left[\mathbf{K}, \mathcal{B}^k = (\bar{e}_1^k, \bar{e}_2^k, \bar{e}_3^k)\right]$ and $\mathcal{F}^\ell = \left[\mathbf{L}, \mathcal{B}^\ell = (\bar{e}_1^\ell, \bar{e}_2^\ell, \bar{e}_3^\ell)\right]$, respectively.

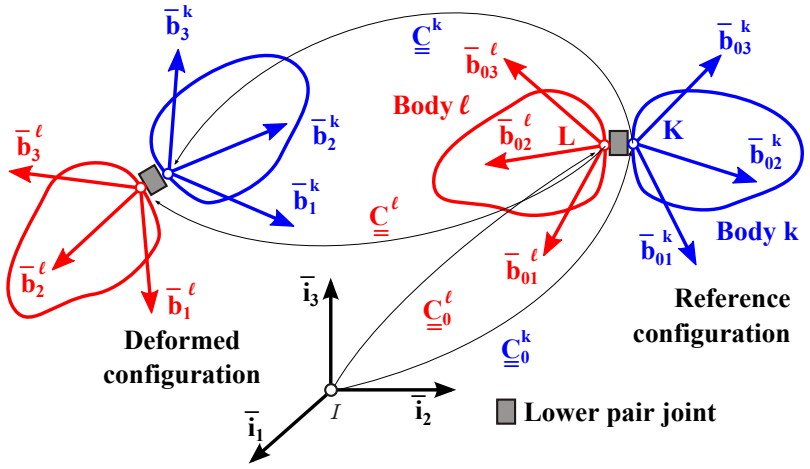

Figure 2: Typical lower pair joint in the reference and deformed configurations.

1.2 Notational conventions

Unless otherwise indicated, the components of all tensors will be resolved in the inertial frame, denoted $\mathcal{F}^I = [\mathbf{O}, \mathcal{I} = (\bar{\imath}_1, \bar{\imath}_2, \bar{\imath}_3)]$. In the reference configuration, the position vectors of points **K** and **L** are denoted $\underline{u}_0^k$ and $\underline{u}_0^\ell$, respectively, and rotation tensors $\underline{\underline{R}}_0^k$ and $\underline{\underline{R}}_0^\ell$ describe the rotations from basis $\mathcal{I}$ to $\mathcal{B}_0^k$ and $\mathcal{I}$ to $\mathcal{B}_0^\ell$, respectively. The displacement vectors of these two points are denoted $\underline{u}^k$ and $\underline{u}^\ell$, respectively; tensors $\underline{\underline{R}}^k$ and $\underline{\underline{R}}^\ell$ describe the rotations from basis $\mathcal{B}_0^k$ to $\mathcal{B}^k$, and $\mathcal{B}_0^\ell$ to $\mathcal{B}^\ell$, respectively. The virtual rotations vectors are defined as $\underline{\delta\psi}^k = \text{axial}(\delta\underline{\underline{R}}^k \underline{\underline{R}}^{kT})$ and $\underline{\delta\psi}^\ell = \text{axial}(\delta\underline{\underline{R}}^\ell \underline{\underline{R}}^{\ell T})$. Finally, the relative displacement vector at the joint is defined as

$$\underline{u} = \underline{u}^\ell - \underline{u}^k. \tag{1}$$

With these notations, unit vectors of triads $\mathcal{B}^k$ and $\mathcal{B}^\ell$ can be expressed as

$$\bar{e}^k_\alpha = \underline{\underline{R}}^k \underline{\underline{R}}^k_0 \bar{\imath}_\alpha \quad \text{and} \quad \bar{e}^\ell_\beta = \underline{\underline{R}}^\ell \underline{\underline{R}}^\ell_0 \bar{\imath}_\beta, \tag{2}$$

respectively, where $\alpha = 1$, 2, or 3 and $\beta = 1$, 2, or 3. Variations of these unit vectors are readily found as

$$\delta\bar{e}^k_\alpha = \tilde{e}^{kT}_\alpha \underline{\delta\psi}^k \quad \text{and} \quad \delta\bar{e}^\ell_\beta = \tilde{e}^{\ell T}_\beta \underline{\delta\psi}^\ell, \tag{3}$$

respectively.

To simplify the expressions of the constraints associated with the various joints, the following notation is adopted for the scalar and vector products of two unit vectors of bases $\mathcal{B}^k$ and $\mathcal{B}^\ell$,

$$g_{\alpha\beta} = \bar{e}^{kT}_\alpha \bar{e}^\ell_\beta, \tag{4a}$$

$$\underline{h}_{\alpha\beta} = \tilde{e}^k_\alpha \bar{e}^\ell_\beta. \tag{4b}$$

Using eqs. (3), variations of these two quantities are easily obtained as

$$\delta g_{\alpha\beta} = (\underline{\delta\psi}^k - \underline{\delta\psi}^\ell)^T \underline{h}_{\alpha\beta}, \tag{5a}$$

$$\delta\underline{h}_{\alpha\beta} = \underline{\delta\psi}^{kT} \underline{\underline{D}}^{k\ell}_{\alpha\beta} - \underline{\delta\psi}^{\ell T} \underline{\underline{D}}^{\ell k}_{\beta\alpha}. \tag{5b}$$

where the following matrices were defined

$$\underline{\underline{D}}^{k\ell}_{\alpha\beta} = \tilde{e}^k_\alpha \tilde{e}^\ell_\beta, \quad \underline{\underline{D}}^{\ell k}_{\beta\alpha} = \tilde{e}^\ell_\beta \tilde{e}^k_\alpha. \tag{6}$$

1.3 Relative motions

In the reference configuration, the relative motions at the joint are assumed to vanish, *i.e.*, $\underline{u}^k_0 = \underline{u}^\ell_0$ and $\underline{\underline{R}}^k_0 = \underline{\underline{R}}^\ell_0$. In the deformed configuration, Δ_γ denote the relative displacement between the two bodies along unit vector $\bar{e}^k_\gamma$, and ϕ_γ the relative rotation about the same unit vector. More formally, the relative displacements and rotations of the two bodies are defined as

$$\bar{e}^{kT}_\gamma \underline{u} - \Delta_\gamma = 0, \tag{7a}$$

$$g_{\alpha\alpha} \sin\phi_\gamma + g_{\alpha\beta} \cos\phi_\gamma = 0, \tag{7b}$$

respectively. In the second equation, indices α, β, and γ, are such that $\epsilon_{\alpha\beta\gamma} = +1$, where $\epsilon_{\alpha\beta\gamma}$ is the permutation symbol. For a planar rotation of magnitude θ about unit vector $\bar{e}^k_\gamma$, $g_{\alpha\alpha} = \cos\theta$, $g_{\alpha\beta} = -\sin\theta$, and eq. (7b) becomes $\sin(\phi_\gamma - \theta) = 0$ or $\phi_\gamma = \theta$, as expected.

Table 1 now formally defines the six lower pairs depicted in fig. 1 in terms of the relative displacement and/or rotation components that each joint allows or inhibits. If the two bodies are rigidly connected to each other, their six relative motions, three displacements and three rotations, must vanish at the connection point.

Setting $\Delta_\gamma = 0$ in eq. (7a) yields the constraint equation expressing the vanishing of the relative displacement along unit vector $\bar{e}^k_\gamma$. Similarly, setting $\phi_\gamma = 0$ in eq. (7b) expresses the vanishing of the relative rotation about unit vector $\bar{e}^k_\gamma$. On the other hand, if relative displacement along unit vector $\bar{e}^k_\gamma$ is allowed, eq. (7a) defines the magnitude of the relative displacement, Δ_γ, along that direction. Similarly, if relative rotation about unit vector $\bar{e}^k_\gamma$ is allowed, eq. (7b) defines the magnitude of the relative rotation, ϕ_γ, about that vector.

The explicit definition of the relative displacement and rotation components in lower pair joints as additional variables represents an important detail of the implementation. First, it allows the introduction of spring and/or damper elements in the joints, as usually required for modeling realistic configurations. Second, the time histories of joint relative motions can be driven according to suitably specified time functions or by actuators presenting their own physical characteristics.

Table 1: Definition of the six lower pair joints. Symbols "✓" or "X" indicate that relative motion is allowed or inhibited, respectively. For the screw joint, p is the pitch of the screw.

	Relative displacements			*Relative rotations*		
Joint type	Δ_1	Δ_2	Δ_3	ϕ_1	ϕ_2	ϕ_3
Revolute	X	X	X	X	X	✓
Prismatic	X	X	✓	X	X	X
Screw	X	X	$p\phi_3$	X	X	✓
Cylindrical	X	X	✓	X	X	✓
Planar	✓	✓	X	X	X	✓
Spherical	X	X	X	✓	✓	✓

2 Generic constraints for lower pair joints

Although the six lower pair joints depicted in fig. 1 are kinematically very different from each other, the constraints they impose on the bodies they are connected to are of two distinct types only. Lower pair joints inhibit one or more relative rotation components, and/or one or more relative displacement components. These two generic constraints are examined in details and the associated forces of constraint are derived from Lagrange's multiplier method in sections 2.1 and 2.2. In addition, the relative rotation and displacement components at a joint will be defined by means of constraint of two types, which are examined in sections 2.3 and 2.4. Once the formulation of these generic constraints has been developed, the formulations of the six lower pair joints will be presented in section 3.

2.1 First constraint: vanishing relative rotation

The constraint associated with the vanishing of the relative rotation at a lower pair joint connecting two bodies is readily obtained by imposing $\phi_\gamma = 0$ in eq. (7b) to find $g_{\alpha\beta} = 0$. In view of eq. (4a), this constraint imposes the orthogonality of two unit vectors, $\bar{e}_\alpha^{kT}\bar{e}_\beta^{\ell} = 0$, and is written in a generic manner as

$$\mathcal{C}_I = g_{\alpha\beta} = \bar{e}_\alpha^{kT}\bar{e}_\beta^{\ell} = 0. \tag{8}$$

For various types of lower pair joints, indices α and β will take different values.

This holonomic constraint is enforced using Lagrange's multiplier method. The potential of the constraint forces is $V_I^c = \lambda_I \mathcal{C}_I$, where λ_I is Lagrange's multiplier used to enforce this constraint; variation of this potential yields $\delta V_I^c = \delta\lambda_I \mathcal{C}_I + \lambda_I \delta\mathcal{C}_I$. The second term represents the virtual work done by the constraint force, $\delta W^c = \lambda_I \delta\mathcal{C}_I = \delta\underline{q}^T \underline{F}_I^c$, where array $\delta\underline{q}$ stores variations of the generalized coordinates associated with this constraint and $\underline{F}_I^c$ the corresponding constraint forces. Variation of the constraint is expressed as $\delta\mathcal{C}_I = \underline{B}_I \delta\underline{q}$, and it follows that $\underline{F}_I^c = \lambda_I \underline{B}_I^T$. Equation (5a) now yields

$$\delta\underline{q} = \begin{Bmatrix} \delta\psi^k \\ \hline \delta\psi^\ell \end{Bmatrix}, \quad \underline{B}_I^T = \begin{Bmatrix} \underline{h}_{\alpha\beta} \\ \hline -\underline{h}_{\alpha\beta} \end{Bmatrix}, \quad \underline{F}_I^c = \lambda_I \underline{B}_I^T. \tag{9}$$

Because the orthogonality constraint expressed by eq. (8) is nonlinear, numerical processes for the solution of constrained multibody systems will rely on successive linearizations of this constraint and associated forces. An increment in the constraint is expressed as

$$\Delta\mathcal{C}_I = \frac{\partial \mathcal{C}_I}{\partial \underline{q}} \Delta\underline{q} = \underline{Z}_I^T \Delta\underline{q}, \tag{10}$$

where array $\underline{Z}_I$ is easily found as

$$\Delta \underline{q} = \begin{Bmatrix} \Delta \underline{\psi}^k \\ \Delta \underline{\psi}^\ell \end{Bmatrix}, \quad \underline{Z}_I = \begin{Bmatrix} \underline{h}_{\alpha\beta} \\ -\underline{h}_{\alpha\beta} \end{Bmatrix}. \tag{11}$$

An increment in the forces of constraint is expressed as

$$\Delta \underline{F}^c_I = \frac{\partial \underline{F}^c_I}{\partial \underline{q}} \Delta \underline{q} = \underline{\underline{X}}_I \Delta \underline{q}, \tag{12}$$

where $\underline{\underline{X}}_I$ is the *equivalent stiffness matrix* for the constraint. Partial derivatives of the constraint forces yield the following expression for this matrix

$$\underline{\underline{X}}_I = \lambda_I \begin{bmatrix} \underline{\underline{D}}^{\ell k}_{\beta\alpha} & -\underline{\underline{D}}^{k\ell}_{\alpha\beta} \\ -\underline{\underline{D}}^{\ell k}_{\beta\alpha} & \underline{\underline{D}}^{k\ell}_{\alpha\beta} \end{bmatrix}, \tag{13}$$

where matrices $\underline{\underline{D}}^{k\ell}_{\alpha\beta}$ and $\underline{\underline{D}}^{\ell k}_{\beta\alpha}$ are defined by eqs. (6).

2.2 Second constraint: vanishing relative displacement

The constraint associated with the vanishing of the relative displacement at a lower pair joint connecting two bodies is readily obtained by imposing $\Delta_\alpha = 0$ in eq. (7a) to find $\bar{e}^{kT}_\alpha \underline{u} = 0$. This constraint imposes the orthogonality of the relative displacement vector defined by eq. (1) to unit vector $\bar{e}^k_\alpha$. This orthogonality constraint is written in a generic manner as

$$\mathcal{C}_{II} = \bar{e}^{kT}_\alpha \underline{u} = 0. \tag{14}$$

For various types of lower pair joints, index α will take different values.

This holonomic constraint is enforced using Lagrange's multiplier method, as discussed in section 2.1. The potential of the constraint forces is $V^c_{II} = \lambda_{II} \mathcal{C}_{II}$, and the virtual work done by the constraint force is $\delta W^c = \delta \underline{q}^T \underline{F}^c_{II}$. The variation of the constraint, $\delta \mathcal{C}_{II}$, is evaluated using eq. (3) to find

$$\delta \underline{q} = \begin{Bmatrix} \delta \underline{u}^k \\ \delta \underline{\psi}^k \\ \delta \underline{u}^\ell \end{Bmatrix}, \quad \underline{B}^T_{II} = \begin{Bmatrix} -\bar{e}^k_\alpha \\ \tilde{e}^k_\alpha \, \underline{u} \\ \bar{e}^k_\alpha \end{Bmatrix}, \quad \underline{F}^c_{II} = \lambda_{II} \underline{B}^T_{II}. \tag{15}$$

An increment in the constraint is expressed as $\Delta \mathcal{C}_{II} = \underline{Z}^T_{II} \Delta \underline{q}$, where array $\underline{Z}_{II}$ is easily found as

$$\Delta \underline{q} = \begin{Bmatrix} \Delta \underline{u}^k \\ \Delta \underline{\psi}^k \\ \Delta \underline{u}^\ell \end{Bmatrix}, \quad \underline{Z}_{II} = \begin{Bmatrix} -\bar{e}^k_\alpha \\ \tilde{e}^k_\alpha \, \underline{u} \\ \bar{e}^k_\alpha \end{Bmatrix}. \tag{16}$$

The equivalent stiffness matrix for this constraint is

$$\underline{\underline{X}}_{II} = \lambda_{II} \begin{bmatrix} \underline{\underline{0}} & \tilde{e}^k_\alpha & \underline{\underline{0}} \\ -\tilde{e}^k_\alpha & \tilde{u}\tilde{e}^k_\alpha & \tilde{e}^k_\alpha \\ \underline{\underline{0}} & -\tilde{e}^k_\alpha & \underline{\underline{0}} \end{bmatrix}. \tag{17}$$

2.3 Third constraint: definition of relative rotation

The constraint associated with the definition of the relative rotation at a lower pair joint connecting two bodies is given by eq. (7b). This constraint is written in a generic manner as

$$\mathcal{C}_{III} = g_{\alpha\alpha} \sin \phi_\gamma + g_{\alpha\beta} \cos \phi_\gamma = 0. \tag{18}$$

Indices α, β, and γ, are such that $\epsilon_{\alpha\beta\gamma} = +1$, where $\epsilon_{\alpha\beta\gamma}$ is the permutation symbol. For various types of lower pair joints, index γ will take different values.

This holonomic constraint is enforced using Lagrange's multiplier method, as discussed in section 2.1. The potential of the constraint forces is $V^c_{III} = \lambda_{III}\mathcal{C}_{III}$, and the virtual work done by the constraint force is $\delta W^c = \delta\underline{q}^T\underline{F}^c_{III}$. The variation of the constraint, $\delta\mathcal{C}_{III}$, is evaluated using eq. (5a) to find

$$\delta\underline{q} = \begin{Bmatrix} \underline{\delta\psi^k} \\ \underline{\delta\psi^\ell} \\ \underline{\delta\phi_\gamma} \end{Bmatrix}, \quad \underline{B}^T_{III} = \begin{Bmatrix} \underline{w} \\ -\underline{w} \\ \tau \end{Bmatrix}, \quad \underline{F}^c_{III} = \lambda_{III}\underline{B}^T_{III}, \tag{19}$$

where $\underline{w} = \underline{h}_{\alpha\alpha}\sin\phi_\gamma + \underline{h}_{\alpha\beta}\cos\phi_\gamma$ and $\tau = g_{\alpha\alpha}\cos\phi_\gamma - g_{\alpha\beta}\sin\phi_\gamma$.

An increment in the constraint is expressed as $\Delta\mathcal{C}_{III} = \underline{Z}^T_{III}\Delta\underline{q}$, where array $\underline{Z}_{III}$ is easily found as

$$\Delta\underline{q} = \begin{Bmatrix} \underline{\Delta\psi^k} \\ \underline{\Delta\psi^\ell} \\ \underline{\Delta\phi_\gamma} \end{Bmatrix}, \quad \underline{Z}_{III} = \begin{Bmatrix} \underline{w} \\ -\underline{w} \\ \tau \end{Bmatrix}. \tag{20}$$

The equivalent stiffness matrix for this constraint is

$$\underline{\underline{X}}_{III} = \lambda_{III}\begin{bmatrix} \underline{\underline{E}}^T & \underline{\underline{E}} & \underline{z} \\ -\underline{\underline{E}}^T & \underline{\underline{E}} & -\underline{z} \\ \underline{z}^T & -\underline{z}^T & -\mathcal{C}_{III} \end{bmatrix}, \tag{21}$$

where $\underline{z} = \underline{h}_{\alpha\alpha}\cos\phi_\gamma - \underline{h}_{\alpha\beta}\sin\phi_\gamma$ and $\underline{\underline{E}} = \underline{\underline{D}}^{k\ell}_{\alpha\alpha}\sin\phi_\gamma + \underline{\underline{D}}^{k\ell}_{\alpha\beta}\cos\phi_\gamma$.

2.4 Fourth constraint: definition of relative displacement

The constraint associated with the definition of the relative displacement at a lower pair joint connecting two bodies is given by eq. (7a). This constraint is written in a generic manner as

$$\mathcal{C}_{IV} = \bar{e}^{kT}_\gamma\underline{u} - \Delta_\gamma = 0. \tag{22}$$

For various types of lower pair joints, index γ will take different values.

This holonomic constraint is enforced using Lagrange's multiplier method, as discussed in section 2.1. The potential of the constraint forces is $V^c_{IV} = \lambda_{IV}\mathcal{C}_{IV}$, and the virtual work done by the constraint force is $\delta W^c = \delta\underline{q}^T\underline{F}^c_{IV}$. The variation of the constraint, $\delta\mathcal{C}_{IV}$, is evaluated using eq. (3) to find

$$\delta\underline{q} = \begin{Bmatrix} \underline{\delta u^k} \\ \underline{\delta\psi^k} \\ \underline{\delta u^\ell} \\ \delta\Delta_\gamma \end{Bmatrix}, \quad \underline{B}^T_{IV} = \begin{Bmatrix} -\bar{e}^k_\alpha \\ \tilde{e}^k_\alpha\,\underline{u} \\ \bar{e}^k_\alpha \\ -1 \end{Bmatrix}, \quad \underline{F}^c_{IV} = \lambda_{IV}\underline{B}^T_{IV}. \tag{23}$$

An increment in the constraint is expressed as $\Delta\mathcal{C}_{IV} = \underline{Z}^T_{IV}\Delta\underline{q}$, where array $\underline{Z}_{IV}$ is easily found as

$$\Delta\underline{q} = \begin{Bmatrix} \underline{\Delta u^k} \\ \underline{\Delta\psi^k} \\ \underline{\Delta u^\ell} \\ \Delta\Delta_\gamma \end{Bmatrix}, \quad \underline{Z}_{IV} = \begin{Bmatrix} -\bar{e}^k_\alpha \\ \tilde{e}^k_\alpha\,\underline{u} \\ \bar{e}^k_\alpha \\ -1 \end{Bmatrix}. \tag{24}$$

The equivalent stiffness matrix for this constraint is

$$\underline{\underline{X}}_{IV} = \lambda_{IV}\begin{bmatrix} \underline{\underline{0}} & \tilde{e}^k_\alpha & \underline{\underline{0}} & \underline{\underline{0}} \\ -\tilde{e}^k_\alpha & \tilde{u}\tilde{e}^k_\alpha & \tilde{e}^k_\alpha & \underline{\underline{0}} \\ \underline{\underline{0}} & -\tilde{e}^k_\alpha & \underline{\underline{0}} & \underline{\underline{0}} \\ \underline{\underline{0}} & \underline{\underline{0}} & \underline{\underline{0}} & \underline{\underline{0}} \end{bmatrix}. \tag{25}$$

3 Constraints for the lower pair joints

In this section, the constraints associated with the six lower pair joints depicted in fig. 1 are detailed. The corresponding constraint forces are derived, and their physical nature is discussed.

3.1 Revolute joints

Figure 2 depicts two bodies linked together by a lower pair joint. The kinematics of the problem and the corresponding notational conventions are presented in sections 1.1 and 1.2, respectively. This section focuses on a specific type of joint, the *revolute joint*, depicted in fig. 3. For this joint, points **K** and **L** are coincident in both reference and deformed configurations. The revolute joint allows the two bodies it connects to rotate with respect to each other about a material axis, selected, by convention, to be $\bar{e}_3^k = \bar{e}_3^\ell$. This condition implies the orthogonality of $\bar{e}_3^k$ to both $\bar{e}_1^\ell$ and $\bar{e}_2^\ell$.

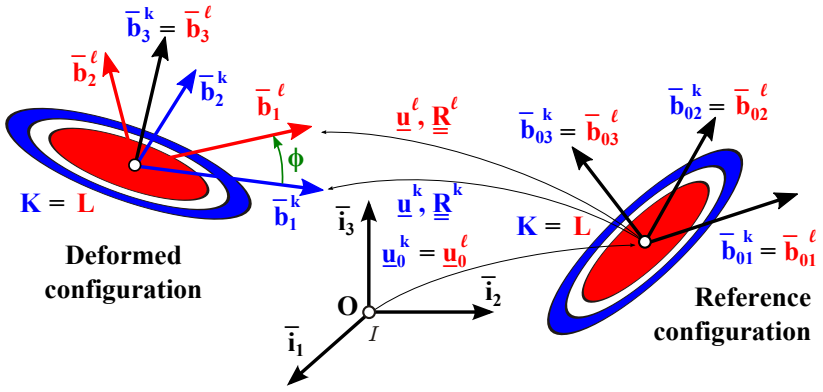

Figure 3: Revolute joint in the reference and deformed configurations.

The revolute joint is characterized by the following kinematic constraints

$$\underline{\mathcal{C}}_1 = \underline{u}^\ell - \underline{u}^k = 0, \tag{26a}$$

$$\mathcal{C}_2 = \bar{e}_3^{kT} \bar{e}_1^\ell = g_{31} = 0, \tag{26b}$$

$$\mathcal{C}_3 = \bar{e}_3^{kT} \bar{e}_2^\ell = g_{32} = 0, \tag{26c}$$

$$\mathcal{C}_4 = g_{11} \sin\phi + g_{12} \cos\phi = 0. \tag{26d}$$

Constraint (26a) expresses the vanishing of the relative displacement at the joint; it is readily enforced by Boolean identification of the corresponding degrees of freedom. The second and third constraints are of type I, see section (2.1), with $\alpha = 3$, $\beta = 1$, and $\alpha = 3$, $\beta = 2$, for eqs. (26b) and (26c), respectively. Finally, the last constraint is of type III, see section 2.3, and defines the relative rotation about unit vector $\bar{e}_3^k = \bar{e}_3^\ell$, denoted ϕ in fig. 3.

The combination of eqs. (9) and (19) yields the forces associated with the revolute joint constraints,

$$\underline{F}^c = \begin{Bmatrix} \underline{h}_{31} \\ -\underline{h}_{31} \\ 0 \end{Bmatrix} \lambda_1 + \begin{Bmatrix} \underline{h}_{32} \\ -\underline{h}_{32} \\ 0 \end{Bmatrix} \lambda_2 + \begin{Bmatrix} (\underline{h}_{11} \sin\phi + \underline{h}_{12} \cos\phi) \\ -(\underline{h}_{11} \sin\phi + \underline{h}_{12} \cos\phi) \\ (g_{11} \cos\phi - g_{12} \sin\phi) \end{Bmatrix} \lambda_3, \tag{27}$$

where Lagrange's multipliers λ_1, λ_2, and λ_3 are associated with constraints (26b), (26c), and (26d), respectively.

When the constraints are satisfied, $\underline{h}_{31} = \bar{e}_2^\ell$ and $\underline{h}_{32} = -\bar{e}_1^\ell$. The forces of constraint associated with the first constraint correspond to two moments acting about unit vector $\bar{e}_2^\ell$ and of magnitudes $+\lambda_1$ and $-\lambda_1$, respectively, applied to bodies k and ℓ, respectively. The forces of constraint

associated with the second constraint are readily interpreted in a similar manner. The moments associated with these first two constraints enforce the parallelism of unit vectors $\bar{e}_3^k$ and $\bar{e}_3^\ell$.

When the constraints are satisfied, $\underline{h}_{11} = \bar{e}_3^k \sin\phi$ and $\underline{h}_{12} = \bar{e}_3^k \cos\phi$, implying that $\underline{h}_{11}\sin\phi + \underline{h}_{12}\cos\phi = \bar{e}_3^k$; furthermore, $g_{11}\cos\phi - g_{12}\sin\phi = \cos\phi\cos\phi - (-\sin\phi)\sin\phi = 1$. To interpret the forces associated with the third constraint, it is assumed that a motor applies a torque Q at the revolute joint; the virtual work done by this torque is then $\delta W = Q\delta\phi$. Because Lagrange's multiplier technique is used to enforce the constraint, the relative rotation, ϕ, is now an unconstrained variable, and the corresponding equation of motion will be $\lambda_3 + Q = 0$: Lagrange's multiplier is of equal magnitude and opposite sign to the applied torque. The remaining components of the constraint forces correspond to two moments acting about unit vector $\bar{e}_3^k$ and of magnitude $-Q$ and $+Q$, respectively, transmitting the applied torque to bodies k and ℓ, respectively. If no torque is applied at the joint, Lagrange's multiplier vanishes, $\lambda_3 = 0$, and no forces are associated with this constraint, which simply defines variable ϕ but applies no forces to the system.

3.2 Prismatic joints

Figure 2 depicts two bodies linked together by a lower pair joint. The kinematics of the problem and the corresponding notational conventions are presented in sections 1.1 and 1.2, respectively. This section focuses on the *prismatic joint*, depicted in fig. 4. For this joint, the two bases coincide in the reference configuration, $\mathcal{B}_0^k = \mathcal{B}_0^\ell$, and in the deformed configuration, $\mathcal{B}^k = \mathcal{B}^\ell$. The prismatic joint allows the two bodies it connects to translate with respect to each other along a material axis, selected, by convention, to be $\bar{e}_3^k = \bar{e}_3^\ell$. This condition implies the orthogonality of unit vectors $\bar{e}_1^k$ and $\bar{e}_2^k$ to the relative displacement vector, $\underline{u} = \underline{u}^\ell - \underline{u}^k$.

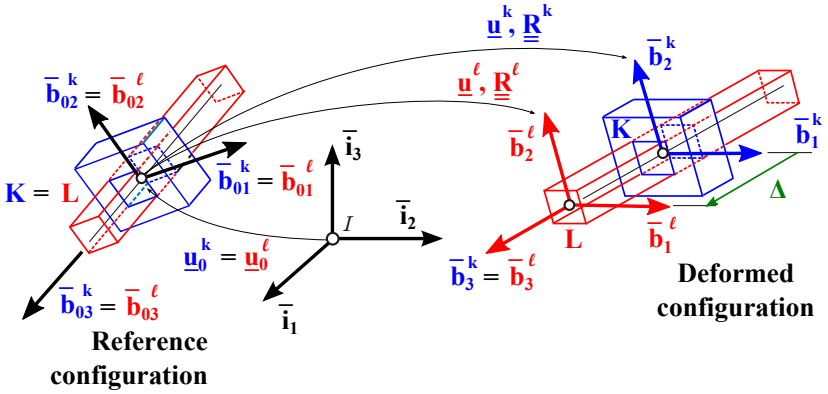

Figure 4: Prismatic joint in the reference and deformed configurations.

The prismatic joint is characterized by the following kinematic constraints

$$\underline{\underline{\mathcal{C}}}_1 = \underline{\underline{R}}^\ell - \underline{\underline{R}}^k = 0, \tag{28a}$$

$$\mathcal{C}_2 = \bar{e}_1^{kT}\underline{u} = 0, \tag{28b}$$

$$\mathcal{C}_3 = \bar{e}_2^{kT}\underline{u} = 0, \tag{28c}$$

$$\mathcal{C}_4 = \bar{e}_3^{kT}\underline{u} - \Delta = 0. \tag{28d}$$

Constraint (28a) expresses the vanishing of the relative rotation at the joint; it is readily enforced by Boolean identification of the corresponding degrees of freedom. The second and third constraints are of type II, see section (2.2), with $\alpha = 1$ and 2, for eqs. (28b) and (28c), respectively. Finally, the last constraint is of type IV, see section 2.4, and defines the relative displacement along unit vector $\bar{e}_3^k = \bar{e}_3^\ell$, denoted Δ in fig. 4.

The combination of eqs. (15) and (23) yields the forces associated with the prismatic joint constraints,

$$\underline{F}^c = \begin{Bmatrix} -\bar{e}_1^k \\ \tilde{e}_1^k \ \underline{u} \\ \bar{e}_1^k \\ 0 \end{Bmatrix} \lambda_1 + \begin{Bmatrix} -\bar{e}_2^k \\ \tilde{e}_2^k \ \underline{u} \\ \bar{e}_2^k \\ 0 \end{Bmatrix} \lambda_2 + \begin{Bmatrix} -\bar{e}_3^k \\ \tilde{e}_3^k \ \underline{u} \\ \bar{e}_3^k \\ -1 \end{Bmatrix} \lambda_3. \tag{29}$$

where Lagrange's multipliers λ_1, λ_2, and λ_3 are associated with constraints (28b), (28c), and (28d), respectively.

When the constraints are satisfied, $\tilde{e}_1^k \ \underline{u} = -\|\underline{u}\|\bar{e}_2^k$, $\tilde{e}_2^k \ \underline{u} = \|\underline{u}\|\bar{e}_1^k$, and $\tilde{e}_3^k \ \underline{u} = 0$. The forces of constraint associated with the first constraint correspond to two forces acting along unit vector $\bar{e}_1^k$ and of magnitude $-\lambda_1$ and $+\lambda_1$, respectively, applied to bodies k and ℓ, respectively, and one moment acting about unit vector $\bar{e}_2^k$ and of magnitude $-\|\underline{u}\|\lambda_1$, applied to both bodies k and ℓ that share a common orientation.

The forces of constraint associated with the second constraint are readily interpreted in a similar manner. The forces associated with these first two constraints enforce the collinearity of unit vectors $\bar{e}_3^k$ and $\bar{e}_3^\ell$; the moments account for the fact that these aligning forces form couples with a moment arm $\|\underline{u}\|$.

To interpret the forces associated with the third constraint, it is assumed that an actuator applies a force F at the prismatic joint; the virtual work done by this force is then $\delta W = F\delta\Delta$. Because Lagrange's multiplier technique was used to enforce the constraint, the relative displacement, Δ, is now an unconstrained variable, and the corresponding equation of motion will be $\lambda_3 - F = 0$: Lagrange's multiplier equals the applied force. The remaining components of the constraint forces correspond to two forces along unit vector $\bar{e}_3^k$ and of magnitude $-F$ and $+F$, respectively, transmitting the applied force to bodies k and ℓ, respectively. If no force is applied at the joint, Lagrange's multiplier vanishes, $\lambda_3 = 0$, and no forces are associated with this constraint.

3.3 Cylindrical joints

Figure 5 depicts the *cylindrical joint*, which is one of the lower pair joints discussed in a generic manner in section 1.1. The cylindrical joint allows the two bodies it connects to rotate and translate with respect to each other about a material axis, implying the orthogonality of $\bar{e}_3^k$ to both $\bar{e}_1^\ell$ and $\bar{e}_2^\ell$ and the orthogonality of unit vectors $\bar{e}_1^k$ and $\bar{e}_2^k$ to the relative displacement vector, $\underline{u} = \underline{u}^\ell - \underline{u}^k$.

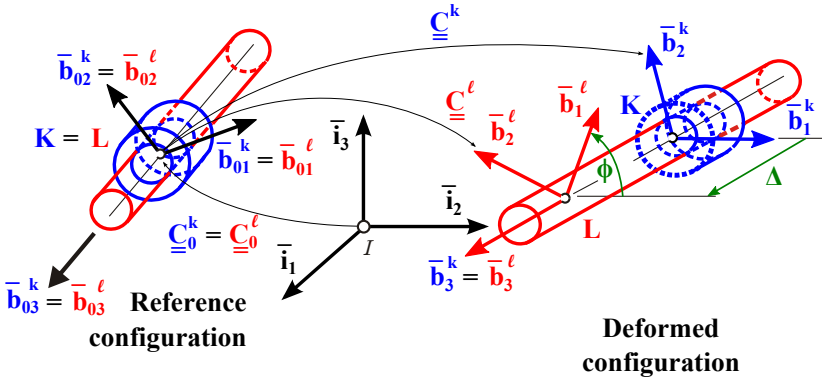

Figure 5: Cylindrical joint in the reference and deformed configurations.

The cylindrical joint is characterized by the following kinematic constraints: constraints (26b) and (26c) expressing the orthogonality of unit vectors $\bar{e}_1^\ell$ and $\bar{e}_2^\ell$ to unit vector $\bar{e}_3^k$, and constraints (28b) and (28c) expressing the orthogonality of unit vectors $\bar{e}_1^k$ and $\bar{e}_2^k$ to the relative displacement vector, $\underline{u}$. The relative rotation about unit vector $\bar{e}_3^k = \bar{e}_3^\ell$, denoted ϕ, and relative

displacement along the same axis, denoted Δ, between the two bodies are defined by adding to the formulation constraints (26d) and (28d), respectively. Clearly, the cylindrical joint combines the constraints of the revolute and prismatic joints. The associated forces of constraints are identical to those developed in section 3.1 and 3.2 and will not be repeated here.

3.4 Screw joints

The kinematic constraints associated with the screw joint are identical to those of the cylindrical joint. An additional constraint imposes a linear relationship between the relative rotation, ϕ, and relative displacement, Δ,

$$\mathcal{C} = \Delta - \frac{p}{2\pi}\phi = 0, \tag{30}$$

where p is the *pitch of the screw*.

3.5 Planar joints

Figure 2 depicts two bodies linked together by a lower pair joint. The kinematics of the problem and the corresponding notational conventions are presented in sections 1.1 and 1.2, respectively. This section focuses on the *planar joint*, depicted in fig. 6. The planar joint allows the two bodies it connects to translate with respect to each other within a material plane, selected, by convention, to be normal to unit vector $\bar{e}_3^k = \bar{e}_3^\ell$. This condition implies the orthogonality of unit vector $\bar{e}_3^k$ to the relative displacement vector, $\underline{u} = \underline{u}^\ell - \underline{u}^k$. The planar joint further allows the two bodies to rotate with respect to each other about the axis perpendicular to the material plane, $\bar{e}_3^k = \bar{e}_3^\ell$. This condition implies the orthogonality of unit vector $\bar{e}_3^k$ to unit vectors $\bar{e}_1^\ell$ and $\bar{e}_2^\ell$.

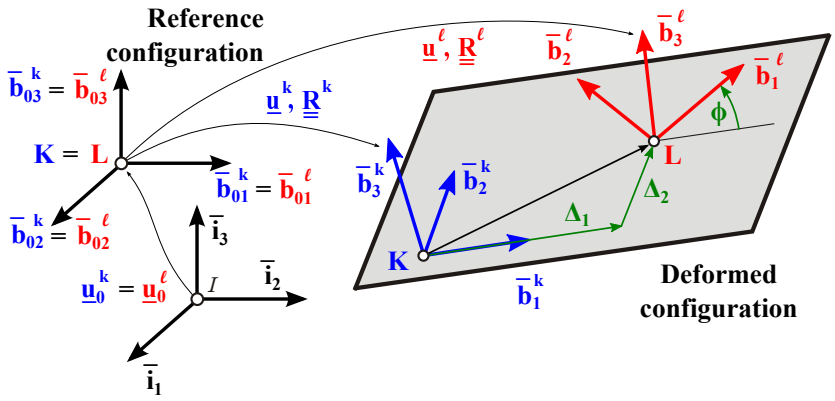

Figure 6: Planar joint in the reference and deformed configurations.

The planar joint is characterized by the following kinematic constraints

$$\mathcal{C}_1 = \bar{e}_3^{kT}\underline{u} = 0, \tag{31a}$$
$$\mathcal{C}_2 = \bar{e}_3^{kT}\bar{e}_1^\ell = g_{31} = 0, \tag{31b}$$
$$\mathcal{C}_3 = \bar{e}_3^{kT}\bar{e}_2^\ell = g_{32} = 0, \tag{31c}$$
$$\mathcal{C}_4 = \bar{e}_1^{kT}\underline{u} - \Delta_1 = 0. \tag{31d}$$
$$\mathcal{C}_5 = \bar{e}_2^{kT}\underline{u} - \Delta_2 = 0. \tag{31e}$$
$$\mathcal{C}_6 = g_{11}\sin\phi + g_{12}\cos\phi = 0. \tag{31f}$$

Constraint (31a) is of type II, see section 2.2, with $\alpha = 3$. The second and third constraints are of type I, see section (2.1), with $\alpha = 3$, $\beta = 1$, and $\alpha = 3$, $\beta = 2$, for eqs. (31b) and (31c), respectively.

The next two constraints are of type IV, see section 2.4, with $\alpha = 1$ and $\alpha = 2$ for eqs. (31d) and (31e), respectively. They define the relative displacements of the bodies along unit vectors $\bar{e}_1^k$ and $\bar{e}_2^k$, respectively, denoted Δ_1 and Δ_2, respectively. Finally, the last constraint is of type III, see section 2.3, and defines the relative rotation about unit vector $\bar{e}_3^k = \bar{e}_3^\ell$, denoted ϕ in fig. 6.

The planar joint combines the constraints of the revolute and prismatic joints. The associated forces of constraints are identical to those developed in sections 3.1 and 3.2.

3.6 Spherical joints

Figure 7 depicts the *spherical joint*, which is one of the lower pair joints discussed in a generic manner in section 1.1. The spherical joint allows the two bodies it connects to freely rotate with respect to each other about a material point, $\mathbf{K} = \mathbf{L}$, while preventing any relative displacement at this point, *i.e.*, $\underline{u}^k = \underline{u}^\ell$.

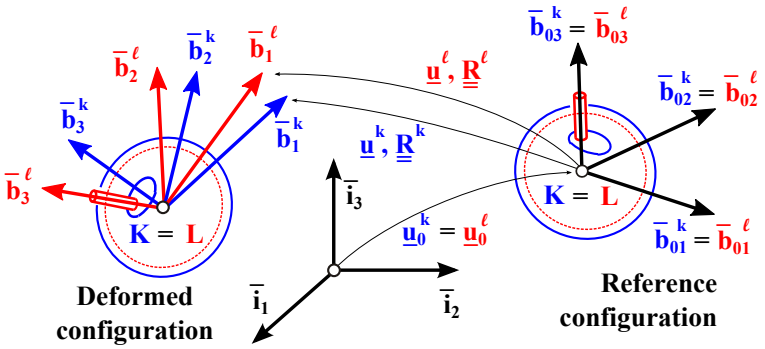

Figure 7: Spherical joint in the reference and deformed configurations.

The spherical joint is characterized by constraints (26a), which prevents relative displacement between the bodies. This constraint is readily enforced by Boolean identification of the corresponding degrees of freedom.

4 Other joints

Multibody systems often involve a variety of joints that impose constraints on the relative motion of the bodies of the system. The lower pairs described in the previous sections can be used to synthesize more complex joints: for instance, the universal joint depicted in fig. 8 can be viewed two revolute joints sharing a common axis of rotation along unit vector $\bar{e}_3^k$ and two more revolute joints sharing a common axis of rotation along unit vector $\bar{e}_3^\ell$. In many cases, however, joints with specialized kinematic conditions must be developed.

4.1 Universal joints

Although the universal joint depicted in fig. 8 is not a lower pair joint, the kinematic description and notational conventions presented in sections 1.1 and 1.2, respectively, will be used here again. At the heart of the universal joint is a cruciform, consisting of two rigidly connected bars assembled together at a 90 degree angle. Body k is allowed to rotate about unit vector $\bar{e}_3^k$, which is aligned with the first bar of the cruciform; body ℓ is allowed to rotate about unit vector $\bar{e}_3^\ell$, which is aligned with the second bar of the cruciform. It follows that unit vectors $\bar{e}_3^k$ and $\bar{e}_3^\ell$ are material axes of bodies k and ℓ, respectively, and point $\mathbf{K} = \mathbf{L}$ is a material point of both bodies.

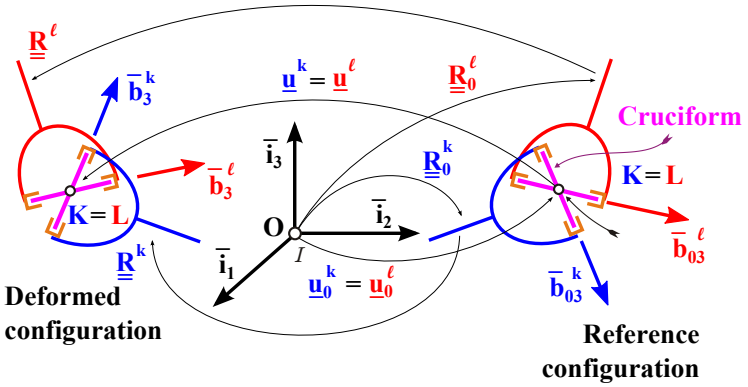

Figure 8: Universal joint in the reference and deformed configurations.

The universal joint is characterized by the following kinematic constraints: constraints (26a), which prevents relative displacement between the bodies, and a single type I constraint, see eq. (8), with $\alpha = \beta = 3$. The universal joint uses a subset of the constraint developed for the revolute joint.

4.2 Constant velocity joints

Although not a lower pair joint, the constant velocity joint is widely used in many mechanism. Numerous different mechanical configurations implement the constant velocity joint. In this section, the non-holonomic constraint associated with the constant velocity joint is presented, without attempting to describe the mechanism by which this constraint is achieved. Figure 9 describes the constant velocity joint; the kinematic description and notational conventions presented in sections 1.1 and 1.2, respectively, will be used here again.

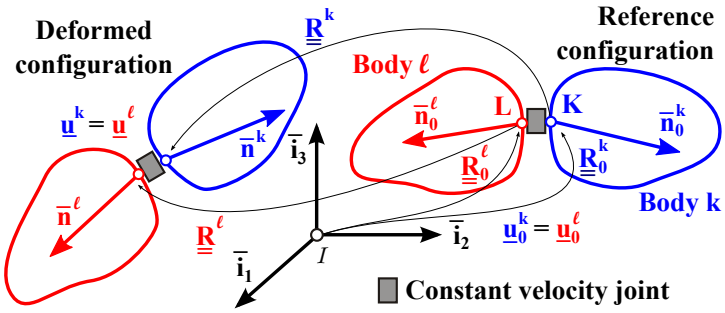

Figure 9: Constant velocity joint in the reference and deformed configurations.

The constant velocity joint connects two bodies, which are attached together at material point $\mathbf{K} = \mathbf{L}$. The rotations of the two bodies are arbitrary, but the projections of their instantaneous velocities along two material directions remain identical at all times. Figure 9 shows two material directions, characterized by unit vectors $\bar{n}_0^k$ and $\bar{n}_0^\ell$ in the reference configurations of bodies k and ℓ, respectively. In the deformed configuration, these material unit vectors are denoted $\bar{n}^k$ and $\bar{n}^\ell$, respectively. The constant velocity constraint is expressed as

$$\bar{n}^{kT} \underline{\omega}^k = \bar{n}^{\ell T} \underline{\omega}^\ell, \tag{32}$$

where $\tilde{\omega}^k = \dot{\underline{\underline{R}}}^k \underline{\underline{R}}^{kT}$ and $\underline{\omega}^\ell = \dot{\underline{\underline{R}}}^\ell \underline{\underline{R}}^{\ell T}$ are the angular velocities of bodies k and ℓ, respectively. Note that constraints (32) are expressed at the velocity level and are not integrable, *i.e.*, they are a non-holonomic constraints.

The constant velocity joint is characterized by the following kinematic constraints: holonomic constraints (26a), which prevent relative displacement between the bodies at point $\mathbf{K} = \mathbf{L}$, and non-holonomic constraints (32).

4.3 Curve sliding joints

The kinematic conditions associated with the sliding of a body along a flexible track have been presented by Li and Likins [2] within the framework of Kane's method. Cardona [3] derived a finite element based formulation for the sliding of a body along a prescribed curve. Finally, Bauchau [4] presented the formulation of a sliding joint that enforces the sliding of a body along a flexible beam. This formulation was later refined [5] to include constraints on the relative rotation between the sliding bodies. This section describes the curve sliding joint that enforces the sliding of a body on a rigid curve connected to another body.

Figure 10 depicts two bodies linked together by a curve sliding joint. Here again, the kinematic description and notational conventions presented in sections 1.1 and 1.2, respectively, will be used. Spatial curve $\mathbb{C}$ is rigidly connected to body k.

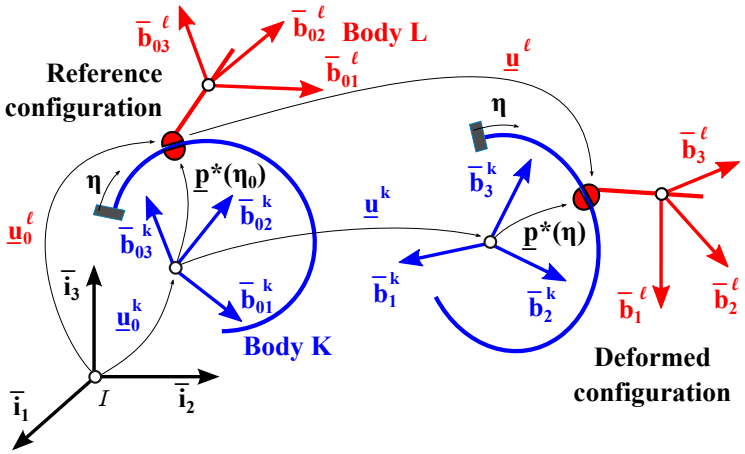

Figure 10: Configuration of the curve sliding joint.

A curve sliding joint involves displacement constraints requiring point $\mathbf{L}$, a material point of body ℓ, to slide along curve $\mathbb{C}$, which is rigidly connected to body k. Let $\underline{p}^*(\eta)$ and $\underline{p}(\eta) = \underline{\underline{R}}^k \underline{\underline{R}}_0^k \underline{p}^*(\eta)$ be the components of the position vector of a point on curve $\mathbb{C}$ with respect to point $\mathbf{K}$, resolved in bases $\mathcal{B}^k$ and $\mathcal{I}$, respectively. Moreover, let $\underline{P}^k$ be the components of the position vector of an arbitrary point on curve $\mathbb{C}$ with respect to point $\mathbf{O}$, resolved in basis $\mathcal{I}$. It then follows that $\underline{P}^k = \underline{u}_0^k + \underline{u}^k + \underline{p}(\eta)$. Similarly, the components of the position vector of point $\mathbf{L}$ with respect to point $\mathbf{O}$, resolved in basis $\mathcal{I}$, are denoted $\underline{P}^\ell = \underline{u}_0^\ell + \underline{u}^\ell$.

Because point $\mathbf{L}$ must be along curve $\mathbb{C}$, the following vector constraint must be satisfied

$$\underline{\mathcal{C}} = \underline{P}^k - \underline{P}^\ell = \underline{u}_0 + \underline{u} + \underline{p}(\eta) = \underline{0}, \tag{33}$$

where $\underline{u}_0 = \underline{u}_0^k - \underline{u}_0^\ell$ and $\underline{u} = \underline{u}^k - \underline{u}^\ell$ are the relative displacement vectors of the two bodies, in the reference and deformed configurations, respectively.

This holonomic constraint is enforced using Lagrange's multiplier method. The potential of the constraint forces is $V^c = \underline{\lambda}^T \underline{\mathcal{C}}$, and the virtual work done by the constraint force is $\delta W^c = \delta \underline{q}^T \underline{F}^c$. The variation of the constraint, $\delta \underline{\mathcal{C}}$, is evaluated as

$$\delta \underline{q} = \begin{Bmatrix} \delta \underline{u}^k \\ \delta \underline{\psi}^k \\ \delta \underline{u}^\ell \\ \delta \eta \end{Bmatrix}, \quad \underline{\underline{B}}^T = \begin{Bmatrix} \underline{\underline{I}} \\ -\tilde{p}(\eta) \\ -\underline{\underline{I}} \\ \underline{p}_1^T(\eta) \end{Bmatrix}, \quad \underline{F}^c = \underline{\underline{B}}^T \underline{\lambda}. \tag{34}$$

where $\underline{p}_1^* = \underline{p}^{*\prime}(\eta)$, $\underline{p}_1(\eta) = \underline{\underline{R}}^k \underline{\underline{R}}_0^k \underline{p}_1^*(\eta)$, and notation $(\cdot)'$ indicates a derivative with respect to η.

It is often necessary to know the curvilinear coordinate, s, along the curves. For instance, if a friction force of magnitude F^f is present between body ℓ and curve $\mathbb{C}$ at point $\mathbf{L}$, the formulation would require the evaluation of the virtual work done by this force, $\delta W = F^f \delta s$. It is often convenient to use the very versatile NURBS representation of curves [6, 7], but this approach is based on an arbitrary parameterization, $\eta \in [0, 1]$. The intrinsic parameterization of the curve directly uses curvilinear coordinate s, but is often very difficult to obtain.

To remedy the situation, an additional scalar constraint relating these two variables is necessary. Expressing the relationship between variables s and η is arduous, and more often that not, impossible. Equation $\dot{s} = p_1 \dot{\eta}$ provides a relationship between the corresponding generalized velocities,

$$\mathcal{C} = \dot{s} - \|\underline{p}_1^*(\eta)\|\dot{\eta} = 0. \tag{35}$$

In general, this constraint is not integrable and hence, must be treated as a nonlinear, nonholonomic constraint.

4.4 Sliding joints

The formulation of prismatic joints was presented in section 3.2. The prismatic joint is characterized by the following kinematic constraints: constraint (28a) that prevents relative rotation between the bodies, and constraints (28b) and (28c) that express the orthogonality of unit vectors $\bar{e}_1^k$ and $\bar{e}_2^k$ to the relative displacement vector $\underline{u}$. Note that although these constraints are expressed in terms of the kinematic variables at points $\mathbf{K}$ and $\mathbf{L}$, they imply the sliding of body ℓ on body k at point $\mathbf{K}$, *when body ℓ is rigid.*

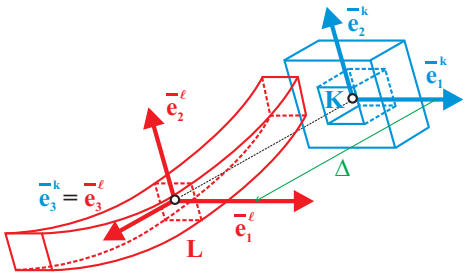

Figure 11: Prismatic joint with flexible body.

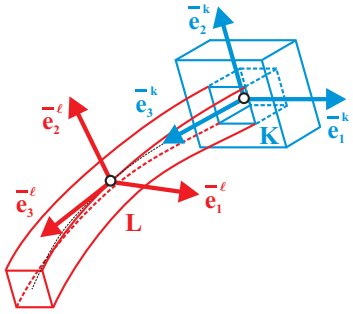

Figure 12: Sliding joint with flexible body.

The situation is sharply different when body ℓ is flexible, as shown in fig. 11. If conditions (28b), (28c) and (28a) are enforced, body ℓ is no longer sliding on body k at point $\mathbf{K}$, *i.e.*, contact between the bodies is no longer enforced. In actual systems, the piece of hardware corresponding to the prismatic joint implies the sliding of body ℓ on body k with contact at point $\mathbf{K}$ at all times, as depicted in fig. 12. In fact, in the presence of flexible bodies, such joint is more accurately described as a *sliding joint* [4, 5, 8].

Due to the flexibility of body ℓ, the kinematic variables at material points $\mathbf{K}$ and $\mathbf{L}$ are no longer related by conditions (28b), (28c) and (28a). Rather, constraint conditions must be enforced between the kinematic variables at point $\mathbf{K}$ of body k, and the kinematic variables at the material point of body ℓ which is in contact with body k at an instant. Clearly, kinematic constraints (28b), (28c) and (28a) associated with the classical formulation of prismatic joints, and the kinematic constraint associated with sliding in the presence of flexible bodies are fundamentally different and will lead to sharply different dynamic responses of the system. Although the above discussion has focused on prismatic joints, it is clear that identical remarks can be made concerning the classical formulation of cylindrical joints, and about their inadequacy to model sliding behavior in the presence of flexible bodies.

Figure 13 depicts two bodies linked together by a sliding joint. Body k is a flexible beam element whose displacement field is interpolated from nodal quantities. In the reference configuration, the coordinates of a point on the beam are

$$\underline{u}_0^k(\eta) = \underline{\underline{N}}(\eta)\underline{\hat{u}}_0^k, \tag{36}$$

where $\underline{\hat{u}}_0^k$ are the nodal positions in the reference configuration, $\underline{\underline{N}}(\eta)$ the displacement interpolation matrix, and $\eta \in [0,1]$ a non-dimensional parameter indicating the location of a material particle along the beam axis in the reference configuration. Body ℓ can be a rigid or flexible element of the system. The position vector of a node point of this body is denoted $\underline{u}_0^\ell$ in the reference configuration.

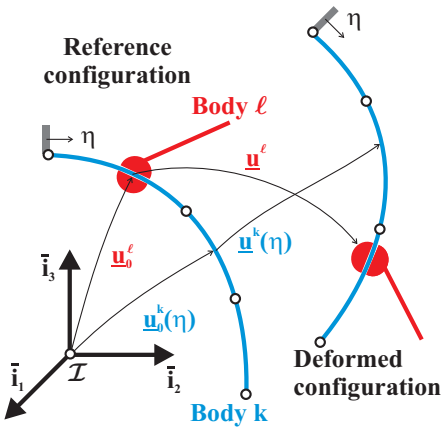

Figure 13: Sliding joint in the reference and deformed configurations.

After deformation, the position vector of a point on the beam becomes $\underline{P}^k(\eta) = \underline{\underline{N}}(\eta)\,(\underline{\hat{u}}_0^k + \underline{\hat{u}}^k)$, where $\underline{\hat{u}}^k$ are the nodal displacement vectors. Similarly, the position vector of the node on body ℓ is $\underline{P}^\ell = \underline{\hat{u}}_0^\ell + \underline{\hat{u}}^\ell$, where $\underline{\hat{u}}^\ell$ is the nodal displacement vector.

The kinematic constraint associated with the condition of body ℓ freely sliding over the flexible beam is $\underline{\mathcal{C}} = \underline{P}^k(\eta) - \underline{P}^\ell = 0$.

Parameter η which determines the location of contact between bodies k and ℓ is, of course, a time varying unknown of the problem. This constraint will be enforced using the Lagrange multiplier method. The virtual work done by the constraint force becomes

$$\begin{Bmatrix} \delta\underline{\hat{u}}^k \\ \delta\eta \\ \delta\underline{u}^\ell \end{Bmatrix}^T \underline{F}^c = \begin{Bmatrix} \delta\underline{\hat{u}}^k \\ \delta\eta \\ \delta\underline{u}^\ell \end{Bmatrix}^T \begin{Bmatrix} \underline{\underline{N}}^T \\ (\underline{\hat{u}}_0^k + \underline{\hat{u}}^k)^T\underline{\underline{N}}'^T \\ -1 \end{Bmatrix} \underline{\lambda}, \tag{37}$$

where $(\cdot)'$ denotes a derivative with respect to η.

References

[1] J. Angeles. *Spatial Kinematic Chains*. Springer-Verlag, Berlin, 1982.

[2] D. Li and P.W. Likins. Dynamics of a multibody system with relative translation on curved, flexible tracks. *Journal of Guidance, Control and Dynamics*, 10:299–306, 1987.

[3] A. Cardona. *An Integrated Approach to Mechanism Analysis*. PhD thesis, Université de Liège, Belgium, 1989.

[4] O.A. Bauchau. On the modeling of prismatic joints in flexible multi-body systems. *Computer Methods in Applied Mechanics and Engineering*, 181(1-3):87–105, 2000.

[5] O.A. Bauchau and C.L. Bottasso. Contact conditions for cylindrical, prismatic, and screw joints in flexible multi-body systems. *Multibody System Dynamics*, 5:251–278, 2001.

[6] L. Piegl and W. Tiller. *The Nurbs Book*. Springer-Verlag, Berlin, New Jersey, second edition, 1997.

[7] G.E. Farin. *Curves and Surfaces for Computer Aided Geometric Design*. Academic Press, Inc., Boston, third edition, 1992.

[8] A. Cardona and M. Géradin. Finite element modeling of flexible tracks. In C. L. Kirk and J.L. Junkins, editors, *Dynamics of Flexible Structures in Space*, pages 411–424. Springer-Verlag, 1990.